Korean J. Chem. Eng., 33(1), 80-89 (2016)
DOI: 10.1007/s11814-015-0095-x

pISSN: 0256-1115
eISSN: 1975-7220

Selective hydrogenation of sunflower oil over Ni catalysts

Emilio Atilano Cepeda, Beatriz Calvo, Irene Sierra, and Unai Iriarte-Velasco†

Department of Chemical Engineering, Faculty of Pharmacy, University of the Basque Country UPV/EHU, Paseo de la Universidad, 7, 01006 Vitoria, Spain
(*Received 25 September 2014 • accepted 12 May 2015*)

Abstract−This work focuses on the influence of the support and the preparation method on the activity and selectivity of nickel catalysts in the hydrogenation of sunflower oil. Catalysts were prepared over silica and alumina supports following the incipient wetness impregnation and deposition-precipitation techniques. The activation process was followed by temperature-programmed reduction (TPR). Precipitation-deposition method allowed a stronger metal-support interaction than incipient wetness impregnation. A precipitation-deposition time of 14 h (which allowed a Ni loading of about 20 wt%) was deemed as the most adequate from the standpoint of high specific surface area and strong Ni-support interaction. The selectivity to oleic acid was not affected by the preparation method, but it was significantly influenced by the type of support. In this regard, the catalysts prepared on silica are more active and produce less saturated fatty acids.

Keywords: Hydrogenation, Vegetable Oil, Nickel, Selectivity, *Trans* Fatty-acids

INTRODUCTION

The hydrogenation of vegetable oils is used in the oils and fats industry to convert polyunsaturated fatty acids into monounsaturated ones. Hydrogenation can be used to improve the flavor stability and to maintain the qualities of oil, especially by reducing the content of highly reactive linoleic acid, thus preventing much of the oxidative rancidity and off-flavor development that might otherwise occur. On the other hand, hydrogenation can change the physical character of oil by turning the liquid into a semisolid, plastic fat, closely resembling butter and suitable for being used in the production of margarine. Other fat/oil applications, such as the production of biolubricants and many renewable chemicals, could also benefit from new advances in catalytic vegetable oil hydrogenation [1-3].

Although only *cis* isomers usually exist in untreated edible oils, during the hydrogenation process some double bonds of the fatty acid chains are isomerized into the *trans* form. There are some growing concerns about the positive associations between the intake of *trans* fatty acids and coronary heart disease. Dietary studies reveal a four- to five-fold higher risk per gram of fatty acids than per gram of saturated fatty acids [3]. Consequently, there has been a trend to favor products with a low *trans* content. The description "low *trans* fatty acid content" implies that the product must contain less than 1% of *trans* fatty acids, with a normally accepted maximum of 0.8% in the finished product. The European Union has recently considered the influence on health of *trans* isomers in foods, and the European Commission is committed to submitting a report on the presence of *trans* fats in foods, accompanied with a legislative frame by December 2014, if appropriate [4]. Therefore, the development of strategies to minimize the production of *trans* isomers during the partial hydrogenation of edible oil has gained much attention. It is well known that the production of *trans* fatty acids depends on various operating conditions, including catalyst type and concentration, mixing intensity, hydrogen pressure and temperature. Among these factors, the most important is the catalyst [5,6].

The hydrogenation process is usually carried out over a catalyst suspended in the liquid oil, and hydrogen is supplied in gas phase. A catalyst supplier is faced with several constraints on the formulation of a catalyst that should exhibit high activity and selectivity for the formation of monoene fatty acids with *cis* configuration and low selectivity to saturated and *trans* fatty acids, as well as low attrition rate. Nickel catalysts are still the most commonly used for vegetable oil hydrogenation [7], since they offer several advantages compared to Pd and Pt catalysts, including high activity and low cost. The use of Ni as promoter in hydrogenation reactions has shown to improve catalyst activity at low hydrogen concentration [8]. In addition, Ni catalysts can be easily removed from processed oil by filtration. To promote the selectivity towards *cis* isomer, different noble metals have been investigated [9,10]. Nevertheless, the influence of the support and the preparation method on catalyst properties and performance has not been investigated in-depth.

The main aim of the present work is to gain insight into the influence of the preparation method and the type of support on the behavior of nickel-containing catalysts in the partial hydrogenation of sunflower oil. Particular emphasis has been placed on the activation of catalysts, which is the least studied aspect in the literature. This work presents results on i) the preparation of nickel catalysts using silica and alumina supports and two preparation methods: incipient wetness impregnation and precipitation-deposition; ii) the activation of the catalysts by temperature programmed reduction and thermogravimetric analysis, in order to draw conclusions

†To whom correspondence should be addressed.
E-mail: unai.iriarte@ehu.eus

about the metal-support interaction and the minimum reduction temperature required; iii) investigation of the performance of the catalysts, focusing on activity and specially, the product distribution of the final product, from a health perspective (amount of *trans* monoenes and saturated stearic acid); and iv) development of a kinetic model that includes the formation of *trans* isomers.

MATERIALS AND METHODS

1. Catalyst Preparation

Two supports were used for the preparation of the catalysts: silica (Köstrosrob 1020, Germany) and commercial γ-Al_2O_3 (Spheralite 511 B, Procatalyse, France). The precipitation-deposition (PD) method is based on the heterogeneous precipitation of nickel from 100 ml of an aqueous solution of 0.14 M nickel nitrate, $Ni(NO_3)_2 \cdot 6H_2O$ (Fluka, p.a.), 0.02 M nitric acid (Probus, p.a.) and 0.42 M urea (Scharlau, p.a.), slurried with 3 g of silica or alumina. The slurry was shaken at 90 °C in a lab-scale rotary evaporator RE 11 (Büchi, Switzerland). The precipitation was produced by the slow and homogeneous change in the pH from 4.6 to 5.5, induced by the thermal decomposition of urea. Samples were then cooled at room temperature, filtered and washed three times with ultrapure water, dried at 110 °C for 14 h in a forced laboratory oven (Memmert, Germany) and calcined at 550 °C for 4 h in a quartz tube furnace (CHESA, Spain).

Regarding the catalyst precursors prepared by the incipient wetness impregnation (IW) method, drops of an aqueous solution of $Ni(NO_3)_2 \cdot 6H_2O$ (Fluka, p.a.) were slowly added to the support under constant agitation. The volume of solution used was equal to the pore volume of the support. The concentration of the solution was that required to obtain the prefixed nickel content. The precursor was dried (110 °C, 14 h) and calcined (550 °C, 4 h).

Prior to use, precursor samples were activated by reduction in a quartz tube furnace. First, the precursors were dried at 150 °C in hydrogen atmosphere for 1 h to remove any trace of water. Afterwards, temperature was raised to the final reduction temperature (550 °C) at a low heating rate (4 °C min^{-1}), to avoid an excessive temperature increase that might badly sinter the catalyst. Finally, samples were kept at 550 °C for 4 h to complete the reduction of the most stable fraction. Due to the pyrophoricity of reduced nickel metal, catalysts were always handled under air-free conditions after the reduction step. These reduction conditions were selected based on the TG and TPR analyses discussed in the results section.

2. Characterization of Catalysts

The nickel content of catalyst precursors was determined by titration with EDTA-murexide, after dissolving them in hydrochloric acid [11].

Specific surface area, average pore diameter and pore volume of supports and catalysts were determined by nitrogen adsorption-desorption at 77 K in an Accusorb 2100E apparatus (Micromeritics, USA). Catalysts were degassed at 150 °C in vacuum prior to surface area measurements.

The thermogravimetric analysis (TG) of precursors was performed by using a thermobalance (SETARAM, France). Samples (40 mg) were heated from room temperature to 800 °C with a heating rate of 10 °C min^{-1} and under a flow of helium of 20 ml min^{-1}. Temperature programmed reduction (TPR) analysis was performed in an AutoChem II 2920 analyzer (Micromeritics, USA) equipped with a thermal conductivity detector (TCD). Temperature was increased from room temperature to 900 °C, at a heating rate of 7.5 °C min^{-1} under a flow of 5% H_2/Ar, and at atmospheric pressure. Prior to analysis samples were subjected to a sweeping treatment with argon at 450 °C for 15 min.

The surface metallic nickel was measured by H_2 pulse chemisorption at 35 °C (Micromeritics Autochem II 2920), after a reduction pretreatment. H_2 consumption was measured by means of a TCD detector. The active surface area of nickel was calculated assuming a molar ratio of $H/Ni_{surf}=1$. The dispersion of nickel was calculated as the ratio between surface nickel and the total loading of nickel.

3. Catalytic Activity Measurements

Experiments were performed using as feedstock a refined commercial sunflower oil (IV. 138.1±0.4) with the following fatty acids composition : palmitic (16 : 0) 6.02±0.12%, stearic (18 : 0) 3.77± 0.08%, oleic (18 : 1) 20.11±0.37%, linoleic (18 : 2) 69.76±0.89%, linolenic (18 : 3) 0.15±0.02% and arachidonic (20 : 0) 0.19±0.03%. Hydrogenation reactions were carried out in a stainless steel reactor operated in a semi-continue mode (105 mm high and 60 mm diameter). The reactor is provided with four baffles to prevent vortex formation, thus allowing an adequate level of turbulence, as proved by previous experiments. The reactor was heated by a PID controlled electric resistance attached to a Pt100 temperature sensor submerged in the liquid. A continuous flow of hydrogen was used, in excess of the stoichiometric amount, to obtain higher yield, as well as reproducible results. A catalyst particle size in the range of 17-80 μm was used to prevent sedimentation and filtration problems.

In a typical hydrogenation run, 75 g of sunflower oil was used. After loading, the reactor was purged with nitrogen to ensure an oxygen-free environment, and the required amount of each catalyst (to yield a fixed Ni to oil ratio) was charged into the reactor. The system was then heated while stirring, and when the reaction temperature was stabilized, hydrogen was introduced into the reactor. The reactor was purged for 15 s to eliminate nitrogen, and then pressure was increased up to the operation value. The time at which the operating pressure was reached was considered to be the initial time. Oil samples were collected for analysis at increasing reaction times.

Refractive indices, measured at 60 °C in an Abbe-Zeiss refractometer (PZO, RL1), were used to monitor the hydrogenation degree. A calibration curve was prepared, to relate the refractive index with the iodine value (IV) of partially hydrogenated oils, measured by the Hanus method.

The fatty acid composition of oil samples was determined by gas chromatography. Reaction products were converted into their methyl esters and analyzed in a 8700 Perkin-Elmer gas chromatograph, equipped with a flame ionization detector (FID) and split-splitless capillary inlet in a 50 m capillary column (Tracsil TR CN100, Tecnokroma). The injector and detector temperatures were 280 and 250 °C, respectively. Hydrogen was used as carrier gas. The oven temperature was kept constant at 80 °C for 6 min, and temperature was then raised to 200 °C at a heating rate of 10 °C min^{-1} and kept 20 min. The total amount of *trans* isomers was obtained by the sum of all C_{18} *trans* isomers.

Table 1. Nickel content and yield of deposition of Ni as a function of precipitation-deposition time

	SiO_2 support		Al_2O_3 support	
Time	Ni (wt%)	Yield (%)	Ni (wt%)	Yield (%)
5 min	<0.1	<0.1	0.03	0.1
1 h	0.3	0.5	0.1	0.2
2.5 h	6.4	11.4	8.3	14.6
5 h	11.7	20.6	12.9	22.8
9 h	14.3	25.2	17.0	30.0
24 h	26.5	46.9	23.0	40.6
34 h	27.7	49.0	25.9	45.8
50 h	28.8	50.9	28.4	50.2
75 h	31.0	54.8	33.1	58.6
100 h	33.0	58.1	35.4	62.6

Table 2. Physical properties of supports and catalyst precursors prepared by precipitation-deposition

Sample	S_{BET} ($m^2\ g^{-1}$)	D_{pore} (Å)	V_{pore} ($cm^3\ g^{-1}$)
SiO_2 support (d_p 17-22 μm)	325	175.0	1.52
$(Ni/SiO_2)_p$ 14.3% Ni	391	69.3	0.68
$(Ni/SiO_2)_p$ 26.5% Ni	390	56.2	0.51
Al_2O_3 support (d_p 40-63 μm)	305	62.0	0.41
$(Ni/Al_2O_3)_p$ 17.0% Ni	256	59.4	0.42
$(Ni/Al_2O_3)_p$ 25.0% Ni	150	52.4	0.32

RESULTS AND DISCUSSION

1. Optimization of the Precipitation-deposition Method

Table 1 shows the results of nickel content and yield of the preparation method, for catalyst precursors prepared using different precipitation-deposition times. The yield was calculated as the ratio between the nickel content of the precursor and the nickel initially available in solution. It is observed that a contact time of 9 h allows high Ni loadings, about 15 wt%. Moreover, from 24 h on the rate of Ni loading is slow (the initial average nickel loading rate is 4% per hour; in the interval of 9-24 h, the rate was 0.8%, and from 24 to 34 h, it decreases to 0.1%). Overall, the precipitation-deposition method allows catalysts with high nickel loading (up to 33 wt%), depending on the precipitation-deposition time.

Table 2 shows the physical properties of supports and catalyst precursors with different Ni loading. Data show that silica support has higher pore volume and pore diameter than alumina support. However, regarding specific surface area little difference is observed between both supports (SiO_2, 325 $m^2\ g^{-1}$; Al_2O_3, 305 $m^2\ g^{-1}$). The decreasing trend in pore diameter with Ni loading can be attributed to the partial blockage of support pores with increasing amounts of deposited metal, as reported by others [12]. Another possible explanation for the decrease in pore size is the degradation/alteration of the porous structure. The reduction in pore size is more pronounced for the samples with the largest pores (silica support), for which a Ni loading of about 25 wt% results in a reduction of 70%. Consequently, for Ni loadings close to 25 wt%, both supports lead to catalyst precursors of comparable pore size and volume.

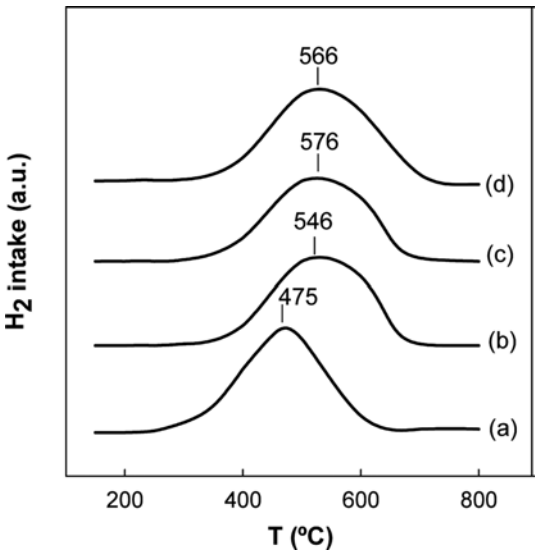

Fig. 1. TPR profiles of nickel catalytic precursors prepared using different precipitation-deposition times. Ni/SiO_2, (a) 5 h; (b) 24 h; (c) 50 h; (d) 100 h.

On the contrary, BET surface area is considerably larger for the sample supported on silica (Ni/SiO_2 26.5%, 390 $m^2\ g^{-1}$ against Ni/Al_2O_3 25.0%, 150 $m^2\ g^{-1}$). This effect, which is attributed to the formation of porous structures of nickel hydrosilicate of high surface area [13], allows an increase of 20% in surface area, up to 390 $m^2\ g^{-1}$. However, for catalyst precursors prepared using Al_2O_3 support, BET surface area decreases with increasing nickel content. This effect may be attributed to the decrease in the percentage of Al_2O_3, which is the main contributor to catalyst surface area. This result suggests either a low dispersion of NiO or the formation of large NiO crystals. Moreover, although nickel hydroaluminate may also be formed, the formation of this phase would take place to a lesser extent. Thus, its contribution to surface area would be lower than in the case of SiO_2 support.

Fig. 1 shows the TPR profiles of catalyst precursors prepared using different precipitation-deposition times, expressed in arbitrary units. All catalyst precursors exhibit one peak at high temperature, related to the reduction of compounds of difficult reducibility. As previously mentioned, nickel hydroxide is expected to react with SiO_2 support to form nickel hydrosilicate, a highly dispersed phase. It is observed that when precipitation-deposition time increases, the maximum intensity value is shifted towards higher temperature, confirming a higher interaction of nickel with SiO_2 support. Similarly, the TPR curves of Ni/Al_2O_3 catalyst precursors show a shift towards lower temperature when precipitation-deposition time increases, up to a time of 24 h. This effect might be explained by the higher Ni content, which results in catalyst precursors more easily reduced. As for silica supported samples, at precipitation-deposition times higher than 24 h, peaks in the TPR curves are shifted towards higher temperatures. This behavior could reflect the formation of low reducibility species such as nickel aluminates at long deposition times. Overall, nickel incorporation causes a higher increase in the temperature required for the reduction when silica is

Table 3. Physicochemical properties of catalysts. PD: catalysts prepared by precipitation-deposition (14 h precipitation-deposition time). IW: catalysts prepared by incipient wetness impregnation

Catalyst	Ni (wt%)	Yield (%)	S_{BET} (m^2 g^{-1})	V_p (cm^3 g^{-1})	D_p (Å)	Ni dispersion (%)
Ni/SiO_2 (PD)	20.4	93.7	395	0.59	62.8	22.8
Ni/Al_2O_3 (PD)	19.1	87.6	235	0.33	54.0	18.2
Ni/SiO_2 (IW)	17.8	49.6	113	0.36	87.8	10.6
Ni/Al_2O_3 (IW)	15.6	64.7	91	0.09	48.7	9.4

used, evidencing a stronger metal-support interaction.

Based on these results, a precipitation-deposition time of 14 h was selected to prepare catalysts with a Ni loading of about 20 wt%, to achieve a compromise between high specific surface area and strong Ni-support interaction. Nickel loading was selected based on the fact that higher nickel contents do not lead to a proportional increase in catalytic activity. Coenen [14] reported that catalyst activity per unit mass of nickel is proportional to accessible nickel surface area, for catalysts of low nickel content (up to 15 wt%, approximately). For higher metallic content, the ratio is not proportional, since part of the nickel is inaccessible, located in small pores. Consequently, only surface nickel determines the reaction rate. Rodrigo et al. [15] confirmed these results using catalysts of low metallic content (10 wt% of nickel onto silica) in the hydrogenation of sunflower oil.

2. Characterization

2-1. Physical Properties

Table 3 shows the nickel content, the preparation yield and the main physical properties of nickel catalysts prepared by PD and IW methods. The Ni content is slightly higher for PD catalysts. Moreover, PD catalysts also show a significantly higher surface area. This effect is not dependent on the support, although it is more pronounced for silica supported catalyst, for which BET area is in-

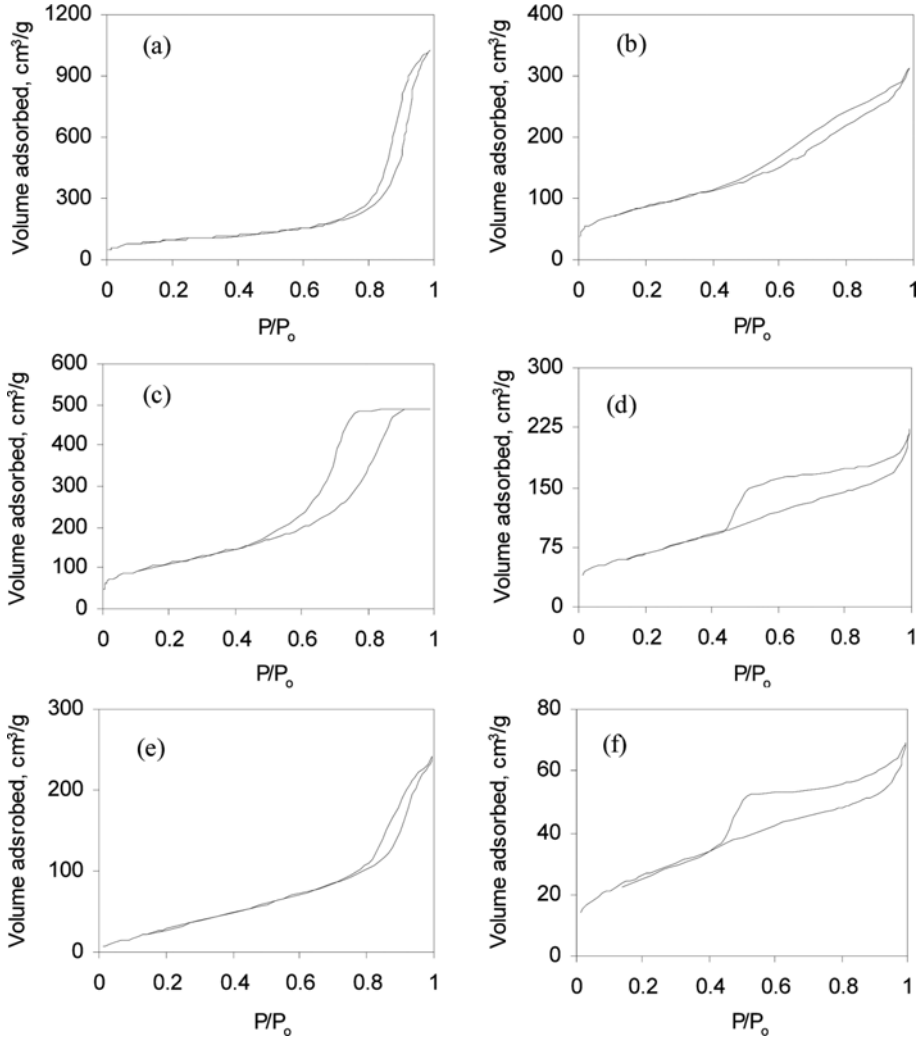

Fig. 2. Nitrogen adsorption-desorption isotherms: (a) SiO_2 support; (b) Al_2O_3 support; (c) Ni/SiO_2 (PD); (d) Ni/Al_2O_3 (PD); (e) Ni/SiO_2 (IW) and (f) Ni/Al_2O_3 (IW).

creased by 250% (395 vs 113 $m^2 g^{-1}$). These results, along with data on Ni dispersion, suggest that the formation of the aforementioned antigorite-like structure (hydrosilicate or hydroaluminate) is favored by PD method compared to IW is favored by PD method compared to IW [13,16]. Ni/SiO_2 (PD) catalyst shows a higher specific surface area than SiO_2 support, reflecting the good nickel-support interaction. A different trend is observed for IW catalysts, for which both specific surface area and pore volume decrease compared to the support (silica or alumina). This phenomenon could be attributed to either pore blockage or to the formation of a disordered mesoporous structure under high nickel content [17].

The nature of the preparation method can lead to different morphologies of Ni nanoparticles. It is known that impregnation leads to larger Ni particles than precipitation-deposition method [18], resulting in a poorer metal dispersion. Data on Ni dispersion shown in Table 3 evidence that precipitation-deposition method results in a higher dispersion of nickel than IW method.

The nitrogen adsorption-desorption experiments conducted for the prepared systems have resulted into comparable profiles of isotherm type IV (Fig. 2), which suggests that the internal porosity of the prepared catalysts is mainly in mesopores and macropores. The hysteresis loops of silica supported catalysts conform to the IUPAC type H1 loops. The isotherm of Ni/SiO_2 (IW) has a shape quite similar to that of SiO_2 support, whereas that of Ni/SiO_2 (PD) exhibits a very different shape, with a much more pronounced hysteresis. The alumina supported catalysts show H2 type hysteresis loops.

The pore size distribution was calculated by BJH method. Fig. 3(a) depicts the incremental pore area of silica-based catalysts. SiO_2 support has a wide pore distribution, with several maximums (148, 200, 247, 322 and 545 Å). Regarding the sample prepared by IW, although there is a considerable reduction of surface area and volume, part of the porous structure still remains. The PSD of Ni/SiO_2 (IW) has one main band with its maximum near 200 Å. Furthermore, this catalyst has another sharp peak at 18 Å. This peak, was not observed for neither support nor Ni/SiO_2 (PD), and evidences the influence of impregnation method in the PSD of the resultant system.

The catalyst prepared by precipitation-deposition shows a very different PSD. It is observed a total suppression of pores larger than 250 Å, due to either pore blockage or degradation. Furthermore, a well defined and sharp peak appears with its maximum at a pore size close to 115 Å. This PSD, along with the value of metallic dispersion (the highest of the four catalysts), suggests the formation of nickel hydrosilicate. This highly dispersed phase compensates for partial pore blockage, resulting in a specific surface area higher than that of the support.

Fig. 3(b) shows the PSD of catalysts prepared onto alumina. Al_2O_3 support has a pore size distribution ranging mainly from 10 to 120 Å. Regarding Ni/Al_2O_3 (IW) catalyst, it shows a noticeable loss of surface area, more pronounced for largest pores. Indeed, the PSD of this catalyst exhibits a unique and well defined peak, with its maximum close to 20 Å. The rest of the porous structure was completely suppressed, as a consequence of pore blockage and/or degradation. The catalyst prepared by precipitation-deposition, on the contrary, displays a large and narrow peak, with its maximum at 22 Å. As occurred with silica support, precipitation-deposition method allows the generation of a highly dispersed structure, as a consequence of the interaction between the metal and the support. When Al_2O_3 is used as a support, the resultant pores are in the 20-60 Å range. This PSD, together with the data of Ni dispersion (higher than that of Ni/Al_2O_3 (IW)), confirms the formation of an antigorite-like structure in Ni/Al_2O_3 (PD) catalyst. However, for Ni/Al_2O_3 catalysts, the formation of this highly dispersed phase is not enough to compensate for the loss of surface area and pore volume. This result confirms that the interaction of nickel with alumina is weaker than with silica, as mentioned in Section 3.1.

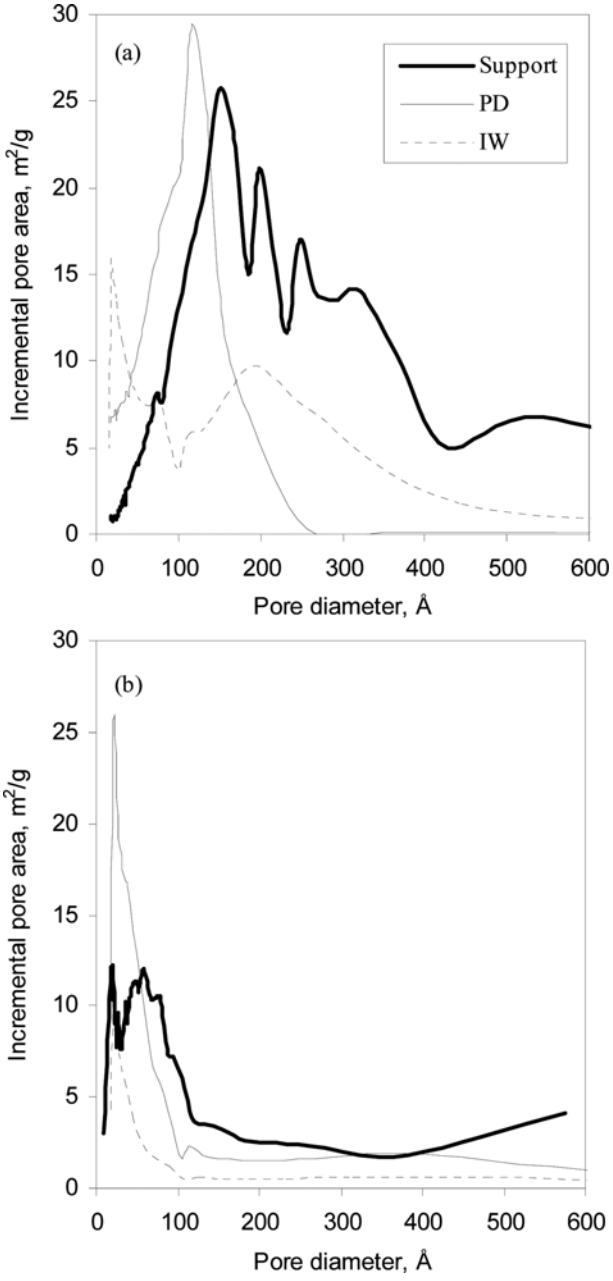

Fig. 3. Pore size distributions: (a) SiO_2 support and catalysts supported on SiO_2; (b) Al_2O_3 support and catalysts supported on Al_2O_3.

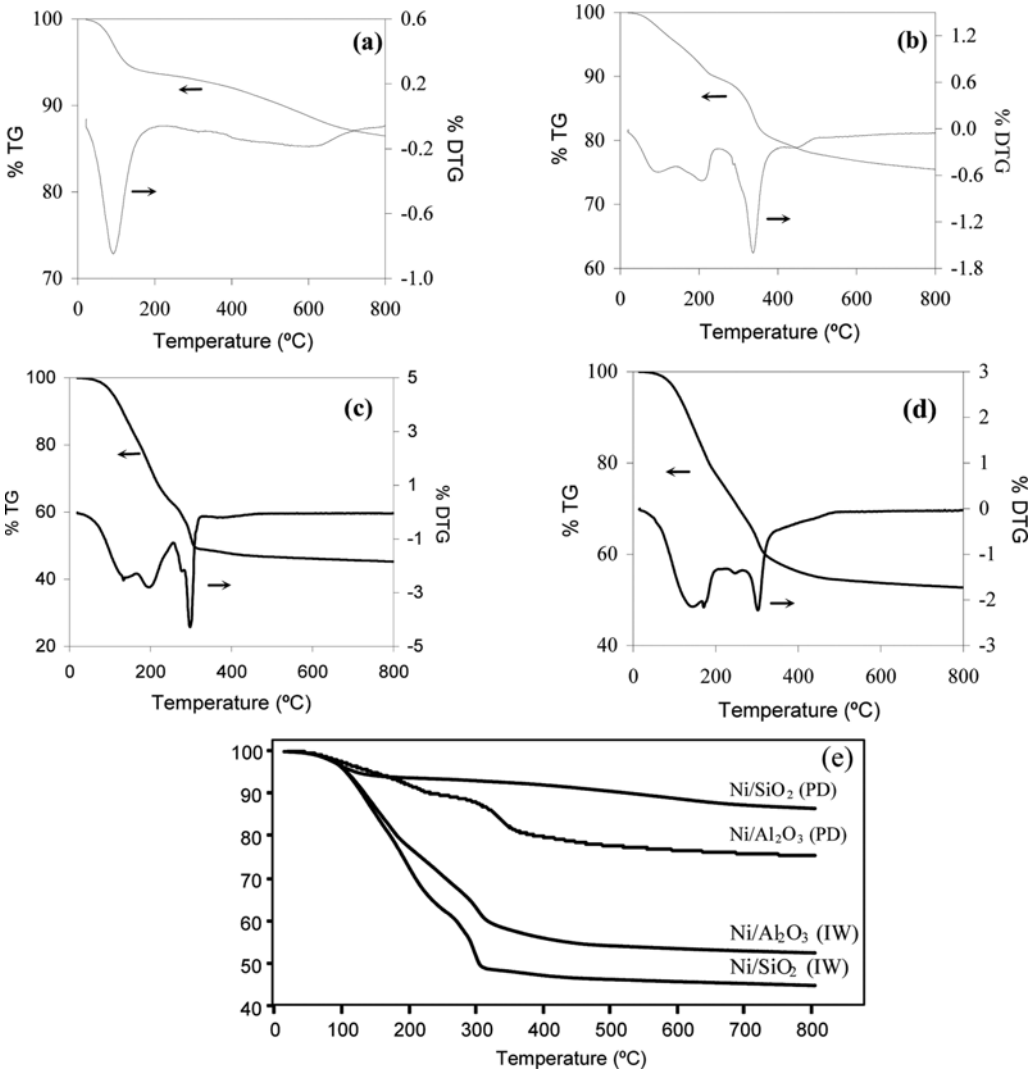

Fig. 4. TG and DTG plots of: (a) Ni/SiO_2 (PD); (b) Ni/Al_2O_3 (PD); (c) Ni/SiO_2 (IW); (d) Ni/Al_2O_3 (IW) and (e) comparison of TG plots for all nickel-containing catalyst precursors.

2-2. Thermogravimetric Analysis

From first derivative TG (DTG) curves (Fig. 4), physically adsorbed water, incorporated in the preparation stage, is removed in the first step of mass loss (peak at 100 °C). The second weight loss (peak at 200 °C) is likely to be related to the removal of hydration water, through the thermal decomposition of the incorporated nickel salts and urea (precipitation catalysts) left behind in the preparation process. The last step (peak at 350 °C) could be ascribed to the decomposition of the deposited $Ni(OH)_2$ to NiO, as well as to the thermal decomposition of residual nickel nitrate.

The aforementioned three peaks appear in the DTG plots of all catalysts, with the exception of Ni/SiO_2 (PD) sample. For this catalyst precursor, only a well defined peak, related to the removal of water at low temperature, is observed. The subsequent weight loss, which takes place gradually up to 650 °C, is attributed to the slow decomposition of nickel phyllosilicate into NiO and SiO_2.

2-3. Temperature Programmed Reduction

Fig. 5 shows the TPR profiles of catalyst precursors. Precursors prepared by IW show two positive peaks at 250 °C and 500 °C, coinciding with the DTG profile. The first peak in IW catalysts may reflect the reduction of supported $Ni(OH)_2$, as well as the reduction of nickel nitrate, left behind in the preparation process. This peak is the main peak for the catalyst supported on silica, whereas for that supported on alumina it appears as a secondary peak. PD catalysts are characterized by a unique broad reduction peak at 500 °C. This result could be explained by the hydrolysis of urea, which has the advantage of increasing the hydroxyl ion concentration. Consequently, PD method leads to a limited nucleation, resulting in a uniform and continuous layer or a homogeneous distribution of small particles over the support suspended in the solution. The higher dispersion of nickel species measured for PD catalysts (Table 3) supports this hypothesis. In general terms, the reduction of nickel takes place at higher temperatures (peak at 550 °C) for PD catalysts, compared to IW catalysts, confirming that the former allows a stronger metal-support interaction.

For the subsequent processes, it was assumed that all NiO can

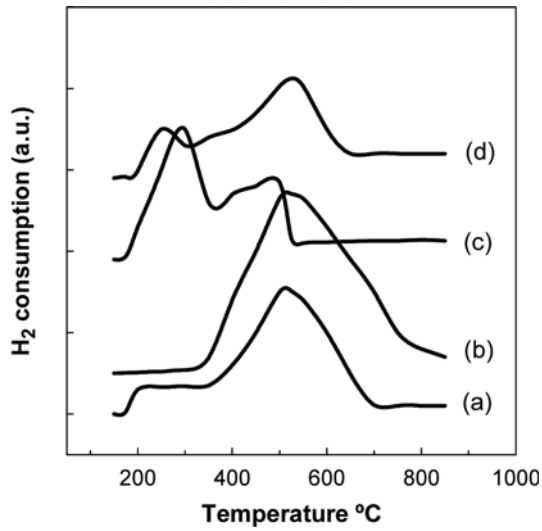

Fig. 5. Temperature programmed reduction (TPR) of nickel catalytic precursors: (a) Ni/SiO_2 (PD); (b) Ni/Al_2O_3 (PD); (c) Ni/SiO_2 (IW); (d) Ni/Al_2O_3 (IW).

be fully reduced to metallic Ni by treating with hydrogen at 550 °C. The selected temperature is in good agreement with the results of other authors [19].

3. Overall Hydrogenation Reaction Rate

A comparative study of sunflower oil hydrogenation was performed using different catalysts (Table 3) under the following reaction conditions: temperature, 150 °C; pressure of hydrogen, 3.5 bar; metal loading, 0.02% Ni/oil. The catalyst particle size was in the 0.010-0.080 mm range. This particle size allows negligible gas-liquid mass-transfer limitations.

Fig. 6 displays the IV decline with reaction time for all four nickel-containing catalysts. The physicochemical properties of the support play a significant role in the reaction rate of the hydrogenation process, which significantly differs among the prepared catalysts. For example, over the course of 2 hours, IV decreases from an initial value of 138 to 10-60 range, depending on the catalyst.

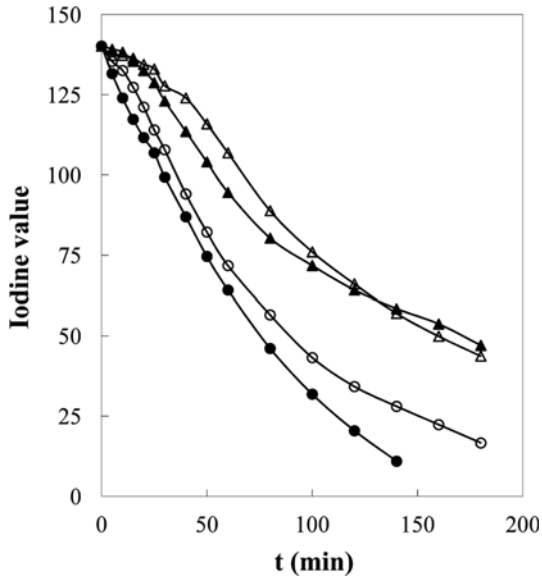

Fig. 6. Evolution with time of iodine value (IV) using different catalysts. (●) Ni/SiO_2 (PD); (▲) Ni/Al_2O_3 (PD); (○) Ni/SiO_2 (IW); (△) Ni/Al_2O_3 (IW).

The hydrogenation activities of these catalysts at the same wt% of metal decreased in the order: Ni/SiO_2 (PD)>Ni/SiO_2 (IW)>Ni/Al_2O_3 (PD)>Ni/Al_2O_3 (IW). Total linoleic conversion is reached after 60 minutes of reaction on silica supported catalysts, whereas for the same time on stream a conversion value of only 70% and 60% is obtained using alumina supported catalysts, PD and IW, respectively.

Consequently, silica supported catalysts exhibit a higher specific activity than alumina supported ones. This result is in good agreement with the aforementioned formation of nickel hydrosilicate, a highly dispersed phase, as observed in TPR plots. Although hydroaluminate could also be formed, it would take place to a lesser extent, thus resulting in a lower dispersion of nickel. Regarding the metal incorporation method, precipitation-deposition leads to more active catalysts than impregnation. As mentioned before, PD method allows a more homogeneous distribution of active sites.

The hydrogenation overall activity follows the same order as pore volume and pore diameter. However, regarding BET surface area no clear trend is observed. Indeed, despite the large BET surface area of Ni/Al_2O_3 (PD) (235 $m^2\ g^{-1}$), its hydrogenation activity is considerably lower than that of Ni/SiO_2 (IW) (113 $m^2\ g^{-1}$). The pores of the support must be large enough so that the active metal is accessible to triglyceride molecules. The oil molecular weight is about 890 g/mol and its diameter about 15 Å considering spherical molecule. This size is close to the pore size of catalysts prepared on porous substrates. The obtained results suggest that a pore diameter three times larger than triglyceride molecular radii ensures an adequate diffusion through the pores of the catalyst and therefore the progress of the reaction. Surface area in the micropore range would not be available for the hydrogenation reaction.

The saturation rate of double bonds was fit to first-order kinetics with respect to the IV decay:

$$\frac{1}{m}\frac{d(IV)_t}{dt} = -k_r(IV)_t \quad (1)$$

where k_r is the overall reaction rate constant expressed on the basis of its specific rate, [(kg of oil)(g of metal)$^{-1}$min^{-1}], m is the metal to oil mass ratio ($g_{metal}\ kg_{oil}^{-1}$) and $(IV)_t$ is the iodine value at a t time. Turnover frequencies (TOF) were calculated from the kinetic rate constant and dispersion data.

The values of the hydrogenation kinetic constant shown in Table

Table 4. Kinetic parameters for catalysts prepared using different supports and preparation methods. Operating conditions: 150 °C and 3.5 bar

Catalyst	% Metal/oil	mk_r (min^{-1})	k_r ($kg_{oil}\ g_{metal}^{-1}\ min^{-1}$)	TOF (min^{-1})
Ni/SiO_2 (PD)	0.021	0.0130	0.0629	1.35
Ni/Al_2O_3 (PD)	0.021	0.0075	0.0351	1.01
Ni/SiO_2 (IW)	0.020	0.0116	0.0574	3.04
Ni/Al_2O_3 (IW)	0.023	0.0064	0.0342	2.33

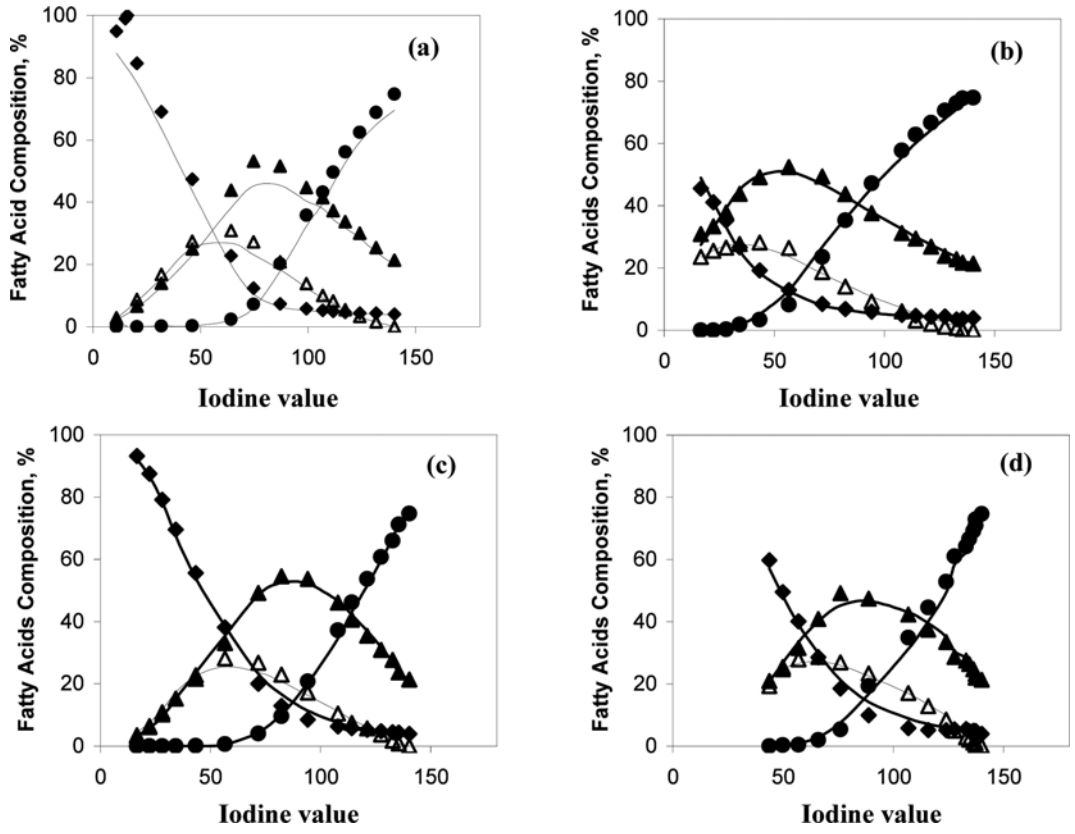

Fig. 7. Reactant and product profile in the hydrogenation of sunflower oil (●) C18:2; (▲) C18:1 *cis*; (△) C18:1 *trans*; (◆) C18:0; (a) Ni/SiO_2 (PD); (b) Ni/Al_2O_3 (PD); (c) Ni/SiO_2 (IW); and (d) Ni/Al_2O_3 (IW). Reaction conditions: temperature, 423 K; H_2 pressure, 3.5 bar, 0.02% Ni/oil. Lines represent model prediction.

4 evidence that silica supported catalysts, at a Ni to oil ratio of about 0.02% (wt/wt), show a significantly higher specific activity than alumina supported ones. Values of k_r range from 0.0574 to 0.0629 kg_{oil} min^{-1} g_{metal}^{-1} and 0.0342 to 0.0351 kg_{oil} min^{-1} g_{metal}^{-1} for silica and alumina supported catalysts, respectively. Regarding the metal incorporation method, PD catalysts show an increase of 10% in k_r values. This enhanced activity is likely to be related to the more homogeneous distribution of active sites observed in TPR plots.

The rates of hydrogenation, expressed as turnover frequency, reveal that accessible atoms of the various Ni catalysts work at varying rate depending on the preparation method. IW catalysts show the largest TOF values where Ni/SiO_2 (IW) shows 2.3 times larger values than the analogous PD system. A similar ratio was measured between the alumina supported systems. Our results reveal that TOF decreases with metal dispersion. A high metal dispersion would increase the proportion of low coordination adsorption sites on which diolefins are strongly adsorbed. The stronger complexation of the metal with the unsaturated hydrocarbons could explain the decrease in TOF values. A similar behavior was reported by others [20] for the hydrogenation of sunflower oil by Pd catalyst supported on alumina, who concluded that the differences in the coordination of sites arising from their location (internal or interfacial) may lead to diversities in the properties of active sites. Furthermore, the enhanced diffusion of reactants through the larger pores of Ni/SiO_2 (IW) could contribute to its increased catalytic efficiency.

4. Kinetic Modeling and Selectivity Analysis

Fig. 7 displays the fatty acid composition profiles. Data show that the *cis*-C18:1 content increases from 20% to 55%, and subsequently decreases to 30%, since double bonds are further saturated, leading to the formation of the saturated stearate (C18:0). Regarding *trans*-C18:1, this component shows a similar trend, with its maximum near 30%, achieved a short time after that of *cis*-C18:1. The stearic acid content remains low (below 10%) up to 40 min of reaction time (reaction extent 40%), and then steadily increases, coinciding with the time at which the maximum *trans*-C18:1 concentration is obtained. Total conversion is achieved after 80 minutes of reaction by using any of the SiO_2 supported catalyst. The shape of the curves is similar for Ni/Al_2O_3 catalysts, although they show less activity.

A kinetic model was developed to describe the evolution of the products during the hydrogenation process. The assumed reaction

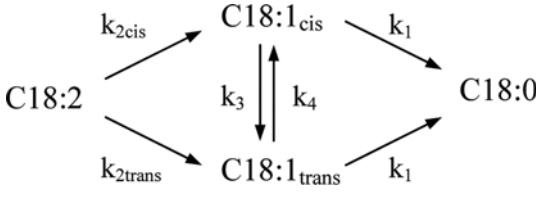

Fig. 8. Reaction pathway described by the kinetic model.

pathway is described in Fig. 8. This model considers the migration of double bonds along the fatty acid chains and *cis-trans* isomerization, which take place simultaneously to the hydrogenation of fatty acids. The model, which is in accordance with others proposed in the literature [21], accounts for the production of *trans* monoenes, compounds of prime importance for the quality of the final product and, therefore, describes more accurately the sunflower oil hydrogenation process.

According to this model, every reaction follows first-order kinetics. In the experimental conditions used in this work, H_2 was fed in excess of the stoichiometric amount. Moreover, the assumption that *cis* and *trans* monounsaturated are equally hydrogenated to the stearate was made.

The methodology used to calculate the evolution of the concentrations consists in solving simultaneously the mass conservation equation for each component and the kinetic equations. The kinetic parameters of best fit were calculated by minimizing the average percentage error (Eq. (2)):

$$APE = \frac{\sum |C_{exp} - C_{pred}| / C_{exp}}{n} \quad (2)$$

where C_{exp} and C_{pred} are the experimental and model predicted concentrations, respectively, and n the number of experimental data.

The calculation of the kinetic parameters was carried out by multivariable nonlinear regression by means of a program written in MATLAB. Lines in Fig. 7 depict the predicted data of fatty acid composition for the four supported nickel-containing catalysts. There is good agreement between experimental and predicted data. Table 5 shows the best fitting kinetic constant values for all four catalysts.

Concerning the performance of the catalysts, it is essential to calculate the selectivity. Several selectivity functions and indices were defined. The traditional overall selectivity, S_I^o, is given by Eq. (3):

$$S_I^o = \frac{k_{2cis}}{k_1} \quad (3)$$

The *trans*-selectivity is a more significant parameter to compare the tendency to form *trans* fatty acids. The proportion of double bonds isomerized to the *trans* configuration relative to those saturated with hydrogen provides a specific isomerization index, expressed as:

$$S_i = \frac{k_3}{mk_r} \quad (4)$$

The production of *cis* monoenes (S_t) may be defined with the S_t index:

$$S_t = \frac{k_{2cis}}{k_3} \quad (5)$$

Table 6. S_I^o selectivity and S_i and S_t indices for nickel catalysts at 150 °C, 3.5 bar and 0.02% Ni/oil

Catalyst	S_I^o	S_i	S_t
Ni/SiO_2 (PD)	5.72	0.041	5.27
Ni/Al_2O_3 (PD)	7.73	0.027	7.39
Ni/SiO_2 (IW)	6.96	0.052	5.17
Ni/Al_2O_3 (IW)	5.06	0.031	6.45

Table 6 summarizes these parameters for the studied catalysts. The values of S_I^o vary from 5.06 to 7.73. According to these values, Ni/Al_2O_3 (PD) and Ni/SiO_2 (IW) catalysts exhibit the highest S_I^o selectivity, reflecting the favorable *cis*-C18:1 formation with respect to the amount of unsaturated fatty acids (C18:0) produced. The opposite could be applied to Ni/SiO_2 (PD) and Ni/Al_2O_3 (IW) catalysts.

The values calculated for S_i range from 0.027 to 0.052. Ni/Al_2O_3 (PD) catalyst, having the highest score in S_I^o shows the lowest value of S_i selectivity, indicating that the parallel isomerization of *cis*-C18:1 to *trans*-C18:1 for a given saturation activity is minimum. This trend to minimize *cis-trans* isomerization is observed for both alumina supported catalyst and could be deemed as a desirable feature of a hydrogenation catalyst. Ni/SiO_2 (IW) catalyst exhibits the highest value of isomerization index, S_i, thus evidencing a higher *trans* fatty acid production. A similar conclusion can be drawn when the catalysts are compared on the basis of the S_t index. Ni/Al_2O_3 catalysts are more effective in reducing the formation of *trans* monoenes, compared to nickel catalysts supported on silica.

The aforementioned selectivity and indices give an overview of the performance of each catalyst over the whole reaction period studied, since they are calculated from the rate of the individual reaction steps. Nevertheless, it is essential to analyze the product distribution corresponding to a target IV level of 70, specially the amount of *trans*-C18:1 and saturated stearic acid, which are of prime importance from the standpoint of the final product quality.

Fig. 9 shows the percentage of *cis* and *trans*-C18:1 and C18:0 at a IV level of 70. This IV value was chosen for two reasons: (i) it is a typical value for oleomargarine, the final product, and (ii) it corresponds to the point at which the formation of stearic acid begins to be important. The lowest amount of *trans* fatty acids is that of Ni/SiO_2 (IW), with a 24.9%, while the highest value corresponds to Ni/Al_2O_3 (PD), with a 26.0%. Regarding the formation of stearic acid (C18:0), Ni/SiO_2 (PD) provides the lowest amount (14.6%) of the catalysts tested (the values for Ni/SiO_2 (IW), Ni/Al_2O_3 (PD) and Ni/Al_2O_3 (IW) are 20.4%, 19.4% and 22.6%, respectively).

Regarding catalyst activity, data in Fig. 6 show that for a target IV value of 70, Ni/SiO_2 systems, either PD or IW, require about half as much reaction time as alumina supported samples (50 min vs. 100 minutes, respectively). Therefore, these catalysts could be

Table 5. Kinetic constant values for nickel catalysts at 150 °C and 3.5 bar

Catalyst	$k_1 \times 10^3$ (min^{-1})	$k_{2cis} \times 10^3$ (min^{-1})	$k_{2trans} \times 10^3$ (min^{-1})	$k_3 \times 10^3$ (min^{-1})	$k_4 \times 10^3$ (min^{-1})	APE (%)
Ni/SiO_2 (PD)	0.49	2.79	1.10	0.53	0.45	8.57
Ni/Al_2O_3 (PD)	0.22	1.70	0.90	0.20	0.20	8.67
Ni/SiO_2 (IW)	0.63	3.10	0.80	0.60	0.30	8.26
Ni/Al_2O_3 (IW)	0.25	1.29	0.70	0.20	0.10	9.28

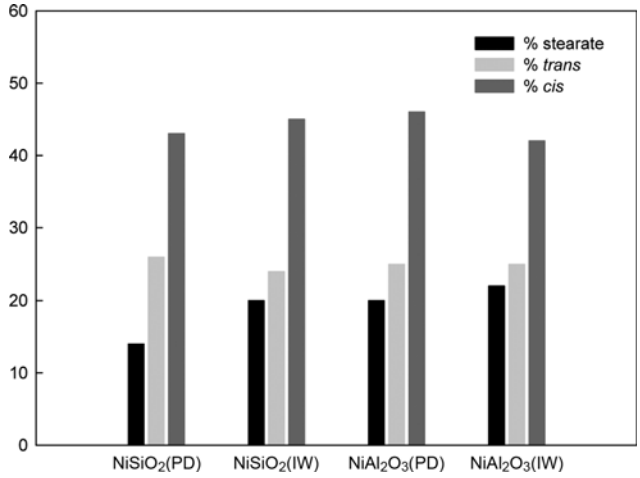

Fig. 9. Percentage of *cis* and *trans* oleate and stearate formed at a IV of 70 for the indicated catalysts.

deemed as the most adequate from both activity and selectivity point of view.

CONCLUSIONS

Several supported nickel catalysts were prepared on silica and alumina, by either precipitation-deposition or impregnation and were tested in the hydrogenation of sunflower oil. Concerning pore diameter, a pore size-to-triglyceride molecular size ratio higher than three for all catalysts ensures an adequate diffusion through the pores and the progress of the reaction.

Regarding the overall hydrogenation rate, catalysts prepared on silica support are more active than those prepared on alumina, probably due to the larger pore size of the former. Also, precipitation-deposition method allows a higher activity than incipient wetness impregnation, due to the stronger metal-support interaction.

When TOF is used as criterion, Ni/SiO_2 (IW) is deemed as the most active catalyst. The turnover frequency is about 2.3-times higher for IW catalysts as compared to PD ones. The differences in the coordination of sites arising from their location may be responsible of higher TOF values.

The kinetic model includes the migration of double bonds along the fatty acid chains and *cis-trans* isomerization. Under mild operating conditions, the model proved to adequately fit the experimental data for the evolution of product distribution with reaction time.

Regarding product selectivity, although the four catalysts result in the formation of significant amounts of *trans* isomers, nickel catalysts prepared on alumina are more selective to *cis* isomers (low S_i and high S_t) than catalysts prepared onto silica. However, at a target IV value of 70, all four catalysts provide a similar amount of *cis* and *trans* monoenes, whereas Ni/SiO_2 (PD) produces less saturated fatty acids.

Based on the obtained results, the Ni/SiO_2 system allows the best performance for sunflower oil hydrogenation. Ni/SiO_2 (PD) catalyst shows the highest overall activity and Ni/SiO_2 (IW) catalyst the highest TOF value. Also, from the standpoint of health and functional properties, Ni/SiO_2 systems could be deemed as good, since they provide adequate selectivity. Ni/SiO_2 (IW) catalyst allows higher overall selectivity, S_l^o, towards *cis* isomer as compared to Ni/SiO_2 (PD), whereas the latter produces the least amount of stearic acid at a target IV value of 70%.

ACKNOWLEDGEMENTS

The authors gratefully acknowledge the financial support for this work provided by the Basque Government (UFI 11/39 (UPV/EHU)). They are also grateful to Prof. A. T. Aguayo (UPV/EHU) for his assistance in catalyst characterization.

REFERENCES

1. F. D. Gunstone, J. L. Harwood and A. J. Dijkstra, 3rd Ed. (2007).
2. F. Zaccheria, R. Psaro, N. Ravasio and P. Bondioli, *Eur. J. Lipid Sci. Technol.*, **114**(1), 24 (2012).
3. K. Lee, C. Hailan, J. Yinhua, Y. Kim and K. Chung, *Korean J. Chem. Eng.*, **25**(3), 474 (2008).
4. Regulation (EU), *Official Journal of theEuropean Union, 343,* **No 1169/2011**, 18 (2011).
5. A. Philippaerts, P. A. Jacobs and B. F. Sels, *Angew. Chem.-Int. Ed.*, **52**(20), 5220 (2013).
6. M. W. Balakos and E. E. Hernandez, *Catal. Today*, **35**(4), 415 (1997).
7. A. J. Dijkstra, *Eur. J. Lipid Sci. Technol.*, **108**(3), 249 (2006).
8. J. Lee, S. Kim, I. Ahn, W. Kim and S. Moon, *Korean J. Chem. Eng.*, **29**(2), 169 (2012).
9. S. McArdle, T. Curtin and J. J. Leahy, *Appl. Catal. A: Gen.*, **382**(2), 332 (2010).
10. S. McArdle, S. Girish, J. J. Leahy and T. Curtin, *J. Mol. Catal. A: Chem.*, **351**(0), 179 (2011).
11. A. Aguinaga, J. C. Delacal, J. M. Asua and M. Montes, *Appl. Catal.*, **51**(1), 1 (1989).
12. P. Burattin, M. Che and C. Louis, *J. Phys. Chem. B*, **103**(30), 6171 (1999).
13. M. A. Ermakova, D. Y. Ermakov, S. V. Cherepanova and L. N. Plyasova, *J. Phys. Chem. B*, **106**(46), 11922 (2002).
14. J. W. E. Coenen, *Ind. Eng. Chem. Fundam.*, **25**(1), 43 (1986).
15. M. T. Rodrigo, L. Daza and S. Mendioroz, *Appl. Catal. A-Gen.*, **88**(1), 101 (1992).
16. L. A. M. Hermans and J. W. Geus, *Stud. Surf. Sci. Catal.*, **2**(3), 113 (1979).
17. W. Cai, L. Ye, L. Zhang, Y. Ren, B. Yue, X. Chen and H. He, *Materials*, **7**(3), 2340 (2014).
18. W. Song, C. Zhao and J. A. Lercher, *Chem. - Eur. J.*, **19**(30), 9833 (2013).
19. C. H. Bartholomew and R. J. Farrauto, *J. Catal.*, **45**(1), 41 (1976).
20. C. Piqueras, S. Bottini and D. Damiani, *Appl. Catal. A: Gen.*, **313**(2), 177 (2006).
21. B. Fillion, B. I. Morsi, K. R. Heier and R. M. Machado, *Ind. Eng. Chem. Res.*, **41**(4), 697 (2002).